

Covariant description of kinetic freeze out through a finite time-like layer

E. Molnar¹, L. P. Csernai^{1,2}, V. K. Magas^{1,3}, Zs. I. Lazar^{1,4}, A. Nyiri¹ and K. Tamasinas¹

¹ Section for Theoretical and Computational Physics,
and Bergen Computational Physics Laboratory,
BCCS-Unifob, University of Bergen,
Allegaten 55, 5007 Bergen, Norway

² MTA-KFKI, Research Inst of Particle and Nuclear Physics,
H-1525 Budapest 114, P.O. Box 49, Hungary

³ Departamento de Física Teórica and IFIC Centro Mixto
Universidad de Valencia-CSIC,
Institutos de Investigación de Paterna
Apdo. correos 22085, 46071, Valencia, Spain

⁴ Department of Physics,
Babes-Bolyai University of Cluj,
Str. M. Kogalniceanu, nr. 1B,
3400 Cluj-Napoca, Romania

Abstract: The Freeze Out (FO) problem is addressed for a covariant FO probability and a finite Freeze Out layer with a time-like normal vector. The resulting post FO momentum distribution functions are presented and discussed. In general the post FO distributions are non-thermal, asymmetric distributions.

PACS numbers: 24.10.Nz, 25.75.-q

I. INTRODUCTION

Freeze out (FO) is a term referring to the stage of expanding or exploding matter when its constituents (particles) lose contact, collisions cease, and local dynamical equilibrium is not maintained. We describe this phenomenon via the example of a relativistic heavy ion collision. In local equilibrium, the evolution of the system can be described by the hydrodynamics, while at the end of the hydrodynamical description the matter freezes out. For p+p reactions this description was first proposed by Landau [1] in the early 1950's.

The hydrodynamical equations are expressions of conservation laws in the presence of continuity and local equilibrium. When the local equilibrium is significantly perturbed, the microscopic length and time scales become comparable to the characteristic macroscopic ones, the hydrodynamical approach breaks down. In the absence of collisions the momentum distribution of the particles freezes out, hence the name kinetic FO.

Starting from the first instant of the hydrodynamical expansion there are particles that leave the interacting system. As time passes the system becomes more dilute, the number of non-interacting particles increases until the whole system breaks up and expands freely without inter-particle collisions. This is the end of the freeze out stage, when the particle momentum is frozen out.

Let us assume the validity of hydrodynamical treatment up to a sharp FO hypersurface, at a constant freeze out temperature. All particle interactions will cease suddenly when reaching the FO temperature, this is a sudden FO process. Thus, the freeze out can be considered as a discontinuity, where the properties of matter change suddenly, across a hypersurface in space-time.

This strong assumption is the limiting case of a more realistic gradual FO process, where the FO description applies over a finite space-time domain, i.e. freeze out layer. Thus, the particles are formed and emitted with different 'temperature' gradually over the expansion volume. However, both descriptions share a common treatment when we are facing the conservation laws.

The properties of the matter are different on the two sides (Pre and Post) of the FO front, but the conservation of baryon charge, energy-momentum and the positive entropy change must hold, thus

$$N_d = 0; \quad T_d = 0; \quad S_d = 0; \quad (1)$$

where the Pre FO baryon and entropy currents and the energy-momentum tensor are $N_0; S_0; T_0$, while the Post FO quantities are $N; S; T$, and the square brackets denote the difference, $[A] = A - A_0$.

As it was shown recently [2], the conservation laws are valid over any surface of discontinuity in relativistic flow. Physically we distinguish two types of hypersurfaces, one with a time-like normal vector ($d \cdot d = 1$), and one with a space-like normal vector ($d \cdot d = -1$). This is important when we calculate nuclear particle spectra, since the widely used method by Cooper and Frye [3] gives a misleading result when it is applied over a FO hypersurface with a space-like normal vector. The solution for this conceptual problem was addressed in recent works [4, 5], resulting in a non-equilibrium cut-off post FO distribution, ensuring that all particles leave the surface only outwards:

$$f_{\text{PostFO}}(\mathbf{x}; \mathbf{p}; d) = f_{\text{PostFO}}(\mathbf{x}; \mathbf{p}) \Theta(d \cdot \mathbf{p}); \quad (2)$$

where both distribution functions depend on particle density, temperature and flow velocity. If we take the

integral of the post FO distribution over the FO hypersurface together with eq. (2), we obtain the (Modified) Cooper-Frye formula:

$$\int_E \frac{dN}{d^3p} = \int_S f_{\text{postFO}}(\mathbf{x}; \mathbf{p}; d) p^0 d^4x; \quad (3)$$

where the phase-space distribution of the frozen out particles is not known from the hydrodynamical model. Thus, it is our task to find the final momentum distribution, to use the correct parameters of the matter and evaluate the FO observables on the post FO side.

The kinetic freeze out model over a finite long space-like and time-like layer was discussed in many recent papers [7, 8, 9, 10]. This paper is partly based on the above mentioned works. A simple kinetic approach is presented in a covariant formalism for a finite time-like layer. The basic philosophy of this paper is similar to the recent paper [11], where the fully covariant treatment is presented for a finite space-like FO layer. In this paper we will generalize the kinetic freeze out treatment for a finite time-like FO layer, and show that our approach can easily handle both space-like and time-like freeze out processes on the same fully covariant footing.

II. FINITE DOMAIN KINETIC FREEZE OUT MODELS

To model the FO mechanism inside a finite space-time layer, we start with some basic assumptions, which can be easily understood following Fig. 1, and the conservation laws across the FO layer.

For start we recall the kinetic definition of the particle four current of conserved charges:

$$N^\mu(\mathbf{x}) = \int \frac{d^3p}{p^0} p^\mu f(\mathbf{x}; \mathbf{p}); \quad (4)$$

where the total number of particles crossing the FO surface in the d direction is:

$$N_S = \int_S N^\mu(x^0) d^3x = \int_S d^3x \int \frac{d^3p}{p^0} p^\mu f(x^0; \mathbf{p}); \quad (5)$$

This expression is valid over any type of 3D time-like hypersurface, while the total number of particles between two parallel hypersurface elements, is

$$\begin{aligned} N_S &= \int_{S_2} N^\mu(x^0) d^3x - \int_{S_1} N^\mu(x^0) d^3x \\ &= \int_{d^4x} ds d^3x \partial_\mu N^\mu(x^0) \\ &= \int_{d^4x} d^4x \int \frac{d^3p}{p^0} \partial_\mu f(x^0; \mathbf{p}) = 0; \end{aligned} \quad (6)$$

where ds is the length element in the direction of freeze out, d^3x is the hypersurface element and

$ds d^3x = d^4x$. Thus, the conservation of the total number of particles requires

$$\partial_\mu N^\mu(\mathbf{x}) = 0; \quad (7)$$

The freeze out of particles starts from the inside boundary of the FO layer, S_1 (thick line). Within the FO layer of finite thickness, L , the density of interacting particles gradually decreases and disappears if we reached the outside boundary, S_2 (thin line), of the FO layer. This can be easily described if we consider two components of the matter, an interacting part plus a free part, thus

$$f(\mathbf{x}; \mathbf{p}) = f_i(\mathbf{x}; \mathbf{p}) + f_f(\mathbf{x}; \mathbf{p}); \quad (8)$$

which for conserved particles leads the following identity

$$N^\mu(\mathbf{x}) = N_i^\mu(\mathbf{x}) + N_f^\mu(\mathbf{x}); \quad (9)$$

If there are no additional particle source or drain terms during the FO process, the conservation of the total particle number, eq. (7) with eq. (9), leads to

$$\partial_\mu N_i^\mu(\mathbf{x}) = -\partial_\mu N_f^\mu(\mathbf{x}); \quad (10)$$

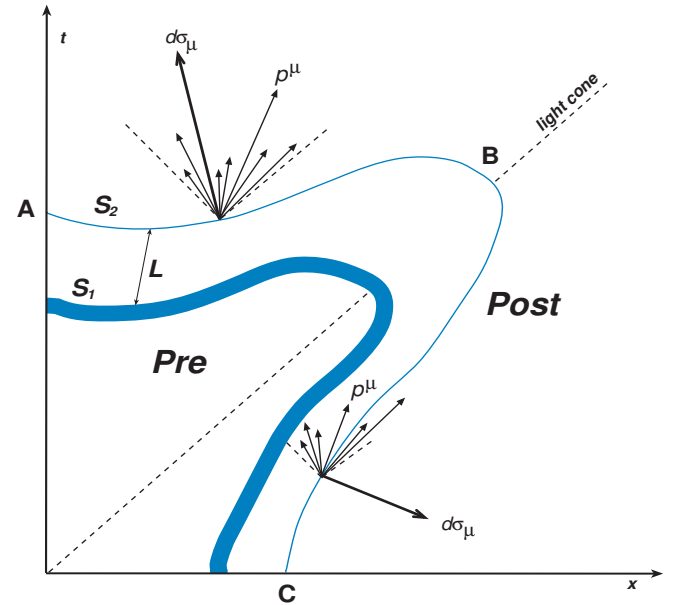


FIG. 1: Between A and B the surface is time-like, from B down to C it is space-like. The momentum of particles is p^μ , the normal to the surface is $d\sigma_\mu$. Along the time-like region all particles emerging from a point belong to the Post FO side, while the particles originating from the space-like part of the FO surface divided between Pre and Post parts. Only those particles cross the surface which have their momentum on the post FO side and the FO surface.

Now, if we write the above equation, eq. (10), in terms of the one particle distribution function, while keeping in

mind that before the freeze out ($t < t_1; x < x_1$), the free component is still non-existent, $f_f(t; x; p) = 0$, therefore

$$\frac{p}{p^0} \partial_t f_i(t; x; p) - (q + v_r) f_i(t; x; p) = 0: \quad (11)$$

In an inhomogeneous system we may always introduce a characteristic length scale, $\lambda_0(x)$, which at a given space point is associated with the inhomogeneity such as:

$$|\nabla_x f_i(x; p)| = f_i(x; p) \frac{1}{\lambda_0(x)}; \quad (12)$$

where $\lambda_0(x)$ represents the typical range, over which the distribution function changes appreciably, see refs. [13, 14]. In an inhomogeneous system, this rate of spatial variation of the one-particle distribution function is related to the local gradients of density and temperature. Now, inserting the above identity into eq. (11), we get

$$\partial_t f_i = -f_i \frac{1}{\lambda_0(x)}; \quad (13)$$

where $\lambda_0 = \lambda_0 = v_j j$ is the characteristic time scale. The sign was chosen in a way that f_i decreases with time.

Furthermore, as time passes the number of interacting particles decreases with the same amount as the number of free particles is increasing. Thus, we find similar equations describing the evolution of the free component as eqs. (12, 13) only with opposite sign.

Before going further, we will write the above equations in a more general form, which can be used in both time-like and space-like cases

$$\frac{p}{p^0} \partial_{\mu} f_i - \frac{1}{p^0} \frac{p^\alpha}{p^s} \frac{d}{dz} \left\{ \frac{d}{dz} \right\} f_i; \quad (14)$$

where s is the coordinate axis in the direction of the FO normal vector, d/dz . Now, the above equation can be applied to any direction normal to the FO surface.¹ Thus, the kinetic equations describing the evolution of both the interacting and free components are

$$\begin{aligned} \partial_s f_i(x; p) ds &= -f_i(x; p) \frac{ds}{\lambda_0(s)}; \\ \partial_s f_f(x; p) ds &= +f_i(x; p) \frac{ds}{\lambda_0(s)}; \end{aligned} \quad (15)$$

where the characteristic mean length, $\lambda_0(x)$, or time, $\lambda_0(t)$, governs the development.

The above form of the kinetic equations were used in recent works [7, 8, 9, 11] to model the FO process over a

space-like layer, while the recent paper [10] for FO with a time-like normal vector.

However, the next step is to approximate the characteristic length, $\lambda_0(s)$, in the above equations. As in ref. [11], we are introducing a so called escape probability,

$$P_{esc} = P_{esc}^1(s); \quad (16)$$

such as this term describes the freeze out or the escape of particles from the interacting component into the free component. In a realistic case the FO probability may depend on the particle density and the momenta. Note that P_{esc} is a probability density!

A qualitative expression of the escape probability can be based on a simple assumption, that the particles with higher escape velocity component have a greater chance to freeze out. This assumption is expressing the momentum, p , dependence of the FO probability. During the FO the interacting particles, which are closer to the outside boundary of the FO layer have a greater chance to freeze out, because the number of interacting particles is decreasing as the FO proceeds. Since the particles are crossing the FO surface only outwards in the direction of the FO normal vector, leads to a non-isotropic space-time dependent FO probability.

The above assumptions are generally valid for a FO description based on a the Boltzmann Transport Equation (BTE). In a realistic approach the FO is finished within a layer of finite thickness, L , which is approximately the length needed for a few collisions. However, we should not forget that generally we have three characteristic scales in a system governed by the kinetic equation, see [13, 14]. There is the correlation length, λ_c or duration of the collision τ_c , followed by an average length or time between the collisions, λ_{or} , which are on microscopic scale, while on the macroscopic scale there is the hydrodynamical length, λ_0 or time λ_0 scale. If the following conditions are satisfied:

$$\lambda_c \ll \lambda_0 \text{ or } \tau_c \ll \lambda_0; \quad (17)$$

then we are in the Boltzmann kinetic regime. However, in different situations, such as high energy heavy ion collisions, there may exist extremely steep temperature and density gradients, i.e. shock waves, detonations, deaggregations. In the special case of freeze out the mean free path becomes very long, much longer than the initial system size. This simply means that we cannot have a complete FO in a finite layer of any thickness smooth enough to be modeled with the BTE. The proposed model, which overcomes the limitations of the BTE approach is the MBTE [6]. Unfortunately, it tends to a very complicated integro-differential equation. Therefore, since the FO description from the first principles is a very complex and time consuming task, it is very important to build a simplified, but nontrivial model, which can help us to understand the basic features of the freeze out process.

Now, we will give a schematic derivation of the escape probability based on the above arguments, however, a

¹

	Time-like	Space-like
∂_s	∂_t	∂_x
p^s	p^0	p^x
$\frac{d}{dz}$	t	x
$\lambda_0(s)$	$\lambda_0(t)$	$\lambda_0(x)$

more detailed treatment of the FO in a finite layer, was presented in ref. [11].

Let us follow a particle, starting from the inner surface of the FO layer, S_2 . This particle is moving orthogonally outwards having the position, x , across the FO layer of finite length. The probability not-to-collide with anything on the way out depends on the number of particles and the remaining distance

$$L - x \quad (18)$$

ahead of us. As this remaining distance becomes smaller the probability to freeze out becomes larger, thus, we may assume that the FO probability is inversely proportional to some power of this quantity [11, 15, 16].

Furthermore, if the particle momentum is not normal to the surface, the spatial distance increases further by $\cos \theta = \frac{p_x}{p} = \frac{p_j}{p}$, where θ is the angle between the FO normal vector, \mathbf{d} , and \mathbf{p} . In our case the FO direction is in the time direction, thus, all the momentum will be represented in the normal FO spectra. Therefore, there is no difference if a particle moves in the positive or in the negative spatial direction, since the particles are freezing out in a time interval at a given spatial point. Particularly, in the case when the FO normal vector is parallel to the flow velocity, the momentum dependent part of the escape probability or the angular factor is unity.

However, we can generalize the angular factor, covering both time-like and space-like hypersurfaces, such as:

$$\cos \theta = \frac{\mathbf{p} \cdot \mathbf{d}}{p u} \quad ; \quad (19)$$

where the detailed analysis of the covariant angular factor can be found in ref. [11, 12].

If we sum up the above assumptions we can approximate the probability for a particle to escape from a time-like layer as:

$$P_{\text{esc}}(\mathbf{x}; \mathbf{p}; \mathbf{d}) = \frac{1}{\tau_0(t)} \quad (20)$$

$$= \frac{1}{L - x} \left(\frac{L}{L - x} \right)^a \left(\frac{p \cdot \mathbf{d}}{p u} \right)^a \quad ;$$

where the power a is influencing the freeze out profile across the layer.

Now, we can generalize the simple model presented in ref. [10] for the finite layer FO with a time-like normal vector following the above made arguments. We choose FO direction to be in the time-direction, thus, eq. (15) will lead to

$$\partial_t f_i = \frac{1}{L - x} \frac{L}{L - x} \frac{p \cdot \mathbf{d}}{p u} f_i \quad ; \quad (21)$$

$$\partial_t f_f = \frac{1}{L - x} \frac{L}{L - x} \frac{p \cdot \mathbf{d}}{p u} f_i \quad ;$$

where a simplified form of the Lorentz invariant escape probability eq. (20) with $(a = 1)$ was used. Solving

the first equation we find that the interacting component deviates from the initial Jüttner shape, $f_J(\mathbf{p})$, as:

$$f_i = f_J(\mathbf{p}) \frac{L}{L - x} \exp\left(-\frac{p \cdot \mathbf{d}}{p u} \frac{x}{L}\right) \quad ; \quad (22)$$

Now, inserting the above result into the second differential equation from eq. (21), leads the momentum distribution of the frozen out particles,

$$f_f = f_J(\mathbf{p}) \frac{f_i}{f_i} \quad (23)$$

$$= f_J(\mathbf{p}) \frac{L}{L - x} \exp\left(-\frac{p \cdot \mathbf{d}}{p u} \frac{x}{L}\right) \quad ;$$

As x tends to the boundary of the FO layer, this distribution will tend to the original Jüttner distribution. This means that the original Jüttner distribution chosen in the beginning survives even if we reached the outer boundary of the FO surface.

To remedy this problem in refs. [7, 8, 9, 10, 11] rethermalization in the interacting component was taken into account. Adding an extra collision term into the description of an inhomogeneous system, will drive the evolution of the system to a state of local equilibrium, see [13, 14].

However, in the special case of FO, only the interacting term is maintaining some level of local equilibrium, thus:

$$\partial_t f_i = \frac{1}{L - x} \frac{L}{L - x} \frac{p \cdot \mathbf{d}}{p u} f_i + \frac{1}{\tau_0} (f_{\text{eq}}(t) - f_i) \quad ;$$

$$\partial_t f_f = \frac{1}{L - x} \frac{L}{L - x} \frac{p \cdot \mathbf{d}}{p u} f_i \quad ; \quad (24)$$

where the interacting component approaches the equilibrated Jüttner distribution, f_{eq} , with τ_0 relaxation time.

Rethermalization within the interacting component happens simultaneously with the freeze out. This is the immediate rethermalization limit, a common simplification, that the local equilibrium is maintained at all times.

A. Reference frames

Before going further, we need to define the possible reference frames, in which our calculations can be done. The properties of the matter are different on the two sides of the FO front, we may denote them as Pre FO and Post FO sides. On the Pre FO side the matter is parameterized by an equilibrium distribution function. The frame where the matter is at rest, i.e. $\mathbf{u} = (1; 0; 0; 0)_{\text{RFG}}$, is the local Rest Frame of the Gas, (RFG), see Fig. 2.

On the Post FO side, the frame which is attached to the freeze out front, i.e. $\mathbf{d} = (1; 0; 0; 0)_{\text{RFF}}$ for the time-like case, is the Rest Frame of the Front, (RFF), see Fig. 2.

Furthermore, there are a few important things to notice. If we are in the RFG frame, i.e. (t, \mathbf{x}) , the flow

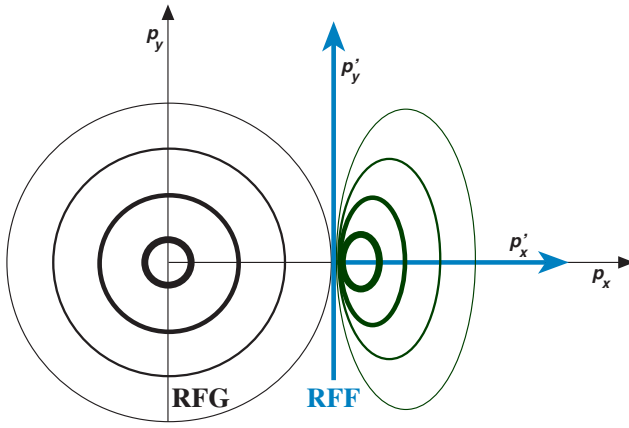


FIG. 2: The different reference frames, RFG and RFF as seen from the RFG, in momentum space. In RFG the initial equilibrium momentum distribution function is spherically symmetric, while in RFF the Post FO momentum distribution is depicted. In case of space-like FO the Post FO distribution function is continued on one hemisphere, as indicated in the figure. In the case of time-like FO the Post FO distribution extends to both hemispheres, but it is generally asymmetric, unless u and d are identical.

velocity is always time-like, $u = (1; 0; 0; 0)_{\text{RFG}}$ in this system. Now, if we take different characteristic points (A, B, C) on the FO hypersurface, then the value of the normal vector, $d = (i; j; k; l)_{\text{RFG}}$, is different at different points of the hypersurface in RFG.

- A) $d = (1; 0; 0; 0)_{\text{RFG}}$, time-like
- B) $d = (1; v; 0; 0)_{\text{RFG}}$.
- C) $d = (1 + \epsilon; 1 - \epsilon; 0; 0)$, just above the light-cone,

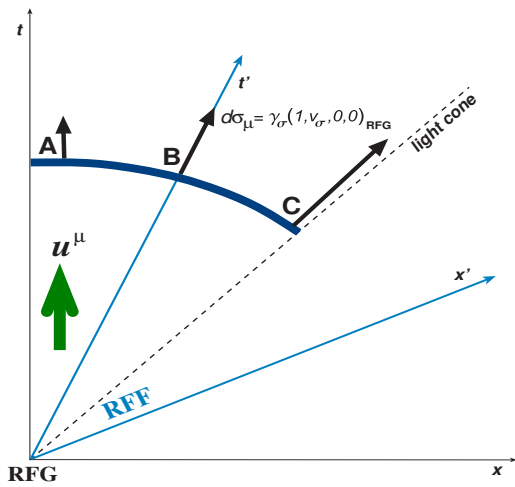


FIG. 3: A simple time-like FO-surface in the Rest Frame of the Gas (RFG: $[t, x]$), where $u = (1; 0; 0; 0)_{\text{RFG}}$. The normal vectors of the FO front, d , are time-like and are plotted at three points: (A, B, C).

To calculate the parameters of the normal vector, d , for different cases listed above in the RFF, we simply make use of the Lorentz transformation. The normal vector of the time-like part of the freeze-out hypersurface may be defined as the local t^0 -axis, while the normal vector of the space-like part may be defined as the local x^0 -axis. This defines the axes of the RFF, where Fig. 3 shows the RFF at point B. However, the four velocity in the RFG will be different in RFF, $u_{\text{RFG}} = (1; v; 0; 0)_{\text{RFF}}$.

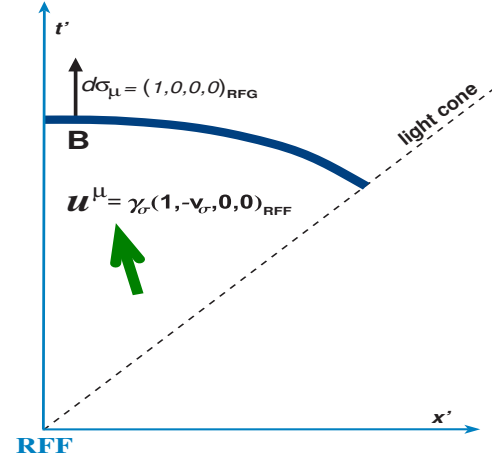


FIG. 4: The same time-like FO surface, which was depicted in Fig. 3 at point B in (RFF: $[t', x']$), where $d = (1; 0; 0; 0)_{\text{RFF}}$ and $u = (1; v; 0; 0)_{\text{RFF}}$.

B. Changes of the conserved current and energy-momentum tensor

The above approach, i.e. to assume that $u = (1; 0; 0; 0)$, will result in a Jüttner type of distribution at all space-time points for the interacting component. Therefore, the equilibrating term in the above equation, eq. (24), can be omitted since it is implicitly taken into account. Thus, only its parameters $T(x)$, $n(x)$ and $u(x)$ need to be determined.

The change of conserved quantities caused by the particle transfer from the interacting matter into the free matter can be obtained in terms of distribution of the interacting matter. The new parameters of the distribution f_i after moving to the right by dt can be obtained from the change in the baryon four current such as:

$$\begin{aligned} dN_i(t) &= dt \int \frac{d^3p}{p^0} p^i \partial_t f_i \\ &= \frac{dt}{L} \int \frac{d^3p}{p^0} p^i \partial_t f_i \\ &= \frac{p^0}{(p^0 - \gamma v p \cos \theta)} f_j(t; p) \end{aligned} \quad (25)$$

and the change in the energy-momentum such as:

$$\begin{aligned} dT_i(t) &= dt \int \frac{d^3p}{p^0} p^i \mathcal{E}_t f_i \\ &= \frac{dt}{L} \int \frac{d^3p}{p^0} p^i \mathcal{E}_t f_i \\ &= \frac{p^0}{(p^0 - \gamma v p_x)} f_i(t; p); \end{aligned} \quad (26)$$

where the four-momentum of particles is $p = (p^0; \mathbf{p})$, $p = \gamma \mathbf{p}$, $p^x = p \cos \theta$, the flow velocity of the interacting matter in RFF is $u_{RFG} = (1; \mathbf{v}; 0; 0)_{RFF}$, $\gamma = \frac{1}{\sqrt{1-v^2}}$, $u = \gamma \mathbf{v}$ and $\mathbf{j} = \text{sign}(\mathbf{v})$.

The general form for the change of conserved particle

density and energy density after a step dt are given in ref. [8, 9]:

$$dn_i(\mathbf{x}) = u_i(\mathbf{x}) dN_i(\mathbf{x}); \quad (27)$$

$$de_i(\mathbf{x}) = u_{,i}(\mathbf{x}) dT_i(\mathbf{x}) + u_i(\mathbf{x}) d\epsilon_i(\mathbf{x}); \quad (28)$$

While these equations are valid in any frame, we can calculate them in the Rest Frame of the Front, RFF, where the values of dN and dT are given below.

The analytical results for the changes of the conserved current and energy-momentum tensor in the case of the time-like calculations are analogous to the calculations for the space-like finite FO layer, see ref. [11].

$$\begin{aligned} dN^0(t) &= \frac{dt}{L} \int \frac{d^3p}{p^0} n \left(G_1^+(\mathbf{p}; m) + G_1(\mathbf{p}; m) \right) \\ &= \frac{dt}{L} \int \frac{d^3p}{p^0} n \frac{(3 + v^2)^2}{3} \\ dN^x(t) &= \frac{dN^0(t)}{\gamma v} \frac{dt}{L} \int \frac{d^3p}{p^0} n \left(\frac{2a}{\gamma v} 2K_1 + aK_0 \right) \\ &= \frac{dt}{L} \int \frac{d^3p}{p^0} n \frac{(3 + v^2)^2}{3v} \frac{1}{v} \\ dT^{00}(t) &= \frac{dt}{L} \int \frac{d^3p}{p^0} \frac{nT}{4} \left(G_2^+(\mathbf{p}; m) + G_2(\mathbf{p}; m) \right) \\ &= \frac{dt}{L} \int \frac{d^3p}{p^0} nT \frac{3(1 + v^2)^3}{3} \\ dT^{0x}(t) &= \frac{dT^{00}(t)}{\gamma v} \frac{dt}{L} \int \frac{d^3p}{p^0} nT \left(\frac{2b^2}{\gamma v} (3 + u^2)K_2 + \frac{2ab^2}{\gamma v} K_1 \right) \\ &= \frac{dt}{L} \int \frac{d^3p}{p^0} nT \frac{3(1 + v^2)^3}{v} \frac{(3 + v^2)}{v} \\ dT^{xx}(t) &= \frac{dT^{0x}(t)}{\gamma v} \frac{T}{\gamma v} \frac{dN^x(t)}{\gamma v} \frac{dN^0(t)}{\gamma v} \frac{dt}{L} \int \frac{d^3p}{p^0} nT \left(\frac{2ab}{u^2} (1 + 3u^2)K_2 + 2ab^2K_1 \right) \\ &= \frac{dt}{L} \int \frac{d^3p}{p^0} nT \frac{3(1 + v^2)^3}{v^2} \frac{(3 + v^2)}{v^2} + \frac{1}{v^2} \frac{(1 + 3v^2)}{v^2} \\ dT^{yy}(t) &= \frac{dT^{xx}(t)}{2} \frac{dt}{L} \int \frac{d^3p}{p^0} \frac{nT}{8} \left(G_3^+(\mathbf{p}; m) + G_3(\mathbf{p}; m) \right) \\ &= \frac{dt}{L} \int \frac{d^3p}{p^0} \frac{nT}{2} dT^{xx}(t) + dT^{00}(t) \end{aligned} \quad (29)$$

$$dT^{zz}(t) = dT^{yy}(t) :$$

where, $a = \frac{m}{T}$, $b = a$, $A(b) = (2 + 2b + b^2)e^{-b}$, $B(b) = \frac{1}{6}(6 + 6b + 3b^2 + b^3)e^{-b}$, $n = 8 T^3 \frac{e^{-\tau}}{(2-\tau)^3}$ and $G_n^+(\rho; m)$, $H_n^+(\rho; m)$, $K_n(a; b)$, $K_n(a)$, $(0; b)$ are defined in the Appendix. The t -dependent factor, $\frac{L}{L-t}$, is just a multiplier in these calculations, and tends to unity if we are dealing with an infinitely long FO, as in ref. [10, 11].

III. RESULTS AND DISCUSSION

Now, we will present our results for the post FO distribution and the relevant quantities from this model, following ref. [11]. The main aim of this work is to compare the finite FO layer results with the infinitely long FO description. All the results are calculated using the Lorentz invariant angular factor, $\frac{p^d}{p^u}$. The difference due to the Lorentz invariance of the angular factor compared with the simple $\cos \theta$, angular factor is small. A brief review of this difference can be found in ref. [11].

We performed calculations for a baryonfree massless gas, similarly to refs. [7, 8]. We have used a simple EoS, $e = s_B T^4$, and with eqs. (27, 28) this results in the set of differential equations:

$$d \ln T = \frac{2}{4 s_B T^4} dT_i^{00} - 2v dT_i^{0x} + v^2 dT_i^{xx} ; \quad (30)$$

$$dv = \frac{3}{4 s_B T^4} v dT_i^{00} + (1 + v^2) dT_i^{0x} - v dT_i^{xx} ;$$

for the changes of the temperature and flow velocity, of the interacting component.

We will present our results for two different cases.

- I) The system is characterized by an infinitely long FO length, ($L \rightarrow 100$). The results are shown, on Figs. (5, 7, 8, 11, 12, 15, 18).
- F) The system is characterized by a finite FO layer, ($L = 10$). The results are shown, on Figs. (6, 9, 10, 13, 14, 16, 19).

The results for the two different cases I and F, listed above are presented in a systematic way on the next set of figures.

1. The evolution of temperature of the interacting component

The first set of figures, Figs. 5 and 6 shows the evolution of temperature of the interacting component in RFF. Comparing Fig. 5 with Fig. 6, we can see the difference between the finite and infinite FO description. We can conclude that in the case of the finite FO layer, the freeze

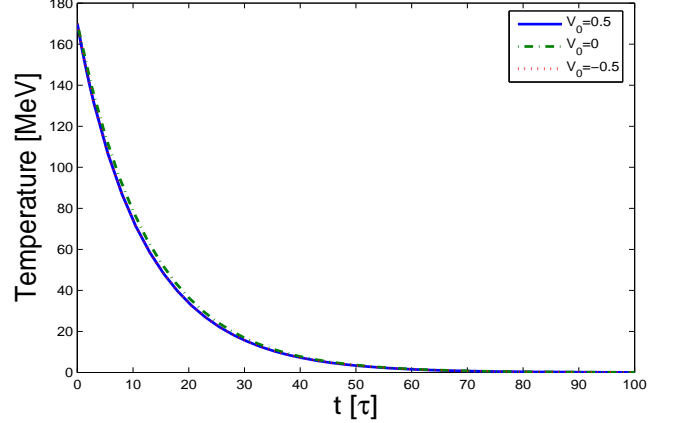


FIG. 5: The temperature of the interacting component in RFF, calculated for an infinitely long, ($L = 100$), FO length. The initial temperature is $T_0 = 170$ MeV, and the parameter, v_0 , is the initial velocity. This corresponds to case I.

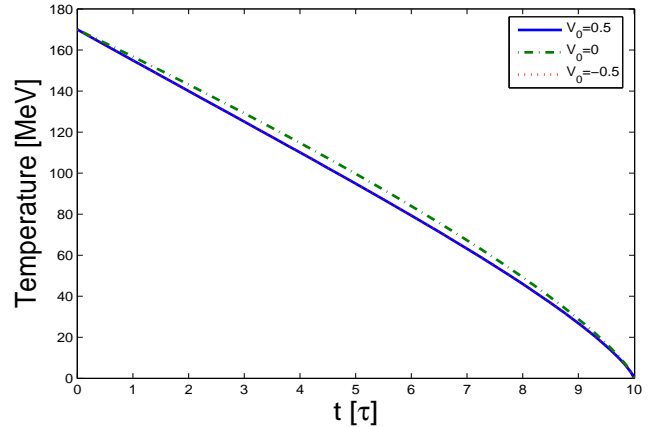


FIG. 6: The temperature of the interacting component in RFF, calculated for a finite ($L = 10$), FO layer. The initial temperature is $T_0 = 170$ MeV, and the parameter, v_0 , is the initial velocity. This corresponds to case F.

out is much faster than in the case of an infinitely long FO description. The temperature curves belonging to different initial flow velocities but with opposite signs are the same. The matter with higher initial flow velocity, v_0 , cools faster, but for small differences between the initial flow velocities, the resulting difference in the temperature is negligible. This is due to the fact that in the case of the time-like FO description we have not apply any constraints on the momenta, i.e. cut-off, (p^d). This can be seen, by comparing the temperature evolution in the space-like FO case, ref. [11].

The final FO temperature is zero, in both cases.

2. The evolution of common flow velocity of the interacting component in RFF and RFG

The second set of figures, Figs. 7, 8, and Figs. 9, 10 shows the evolution of the flow velocity in RFF and RFG respectively.

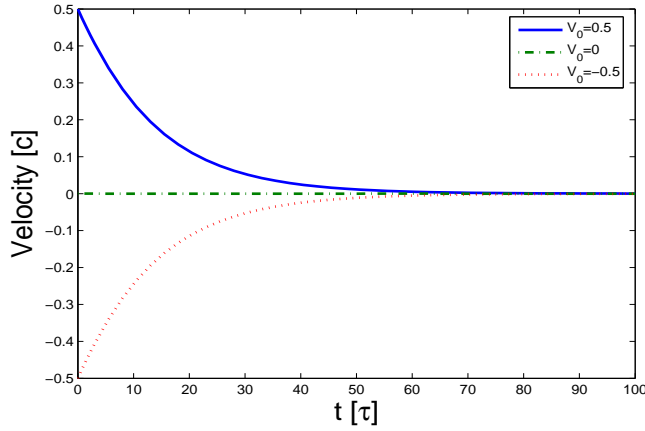


FIG. 7: The evolution of the flow velocity of the interacting component for a baryon-free massless gas, calculated for an infinitely long ($L = 100$), FO length. The initial temperature is $T_0 = 170M$ eV. The parameter, v_0 , is the initial velocity, in RFF. This corresponds to case I.

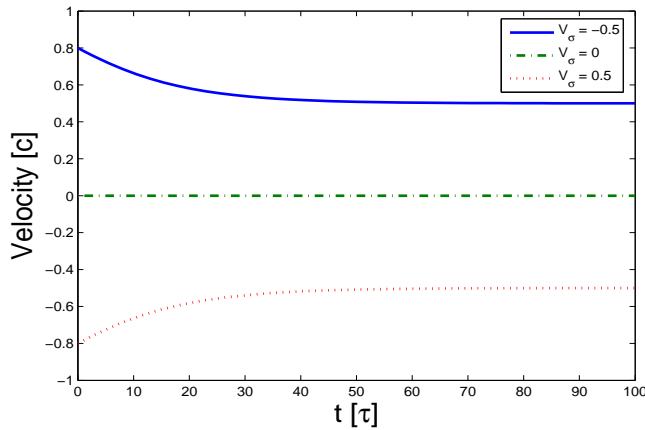


FIG. 8: The evolution of the flow velocity of the interacting component for a baryon-free massless gas, calculated for an infinitely long ($L = 100$), FO length. The initial temperature is $T_0 = 170M$ eV. The parameter, v , is the initial flow velocity, in RFG. The flow parameter, v , is in the direction of d , where $d = (1; v; 0; 0)$.

First, comparing Fig. 7 with Fig. 9, we can see the difference between the finite and infinite FO description. We can conclude that in the case of the finite FO layer, velocity decrease is much faster than in the case of an infinitely long FO description.

Furthermore, comparing Fig. 7 with Fig. 8 or Fig. 9 with Fig. 10 we notice that in case of time-like FO the

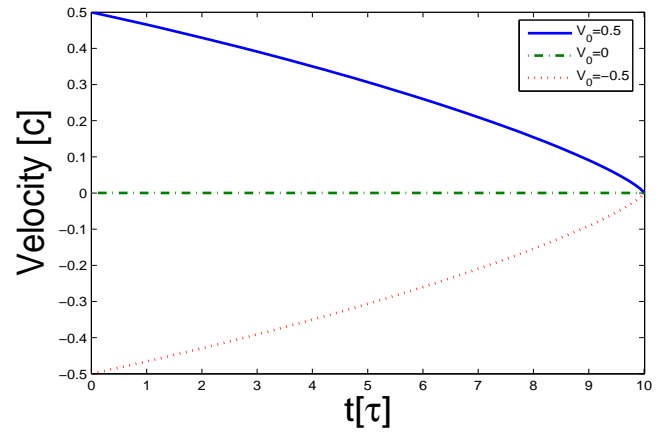


FIG. 9: The evolution of the flow velocity of the interacting component for a baryon-free massless gas, calculated for a finite ($L = 10$), FO length. The initial temperature is $T_0 = 170M$ eV. The parameter, v_0 , is the initial velocity, in RFF. This corresponds to case F.

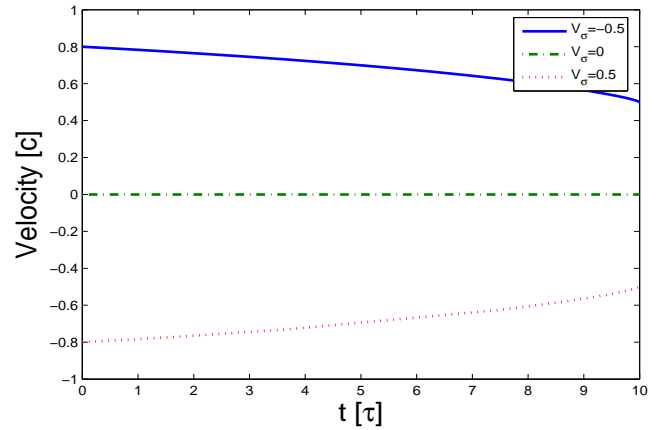


FIG. 10: The evolution of the flow velocity of the interacting component for a baryon-free massless gas, calculated for a finite ($L = 10$), FO length. The initial temperature is $T_0 = 170M$ eV. The parameter, v , is the initial flow velocity, in RFG. The flow parameter, v , is in the direction of d , where $d = (1; v; 0; 0)$.

common flow velocity of interacting component tends to zero, while in case of space-like FO it tends to 1, (see ref. [11]). This is an artifact of the reference frame of the front, RFF, which behaves discontinuously at the light cone. In the rest frame of the gas, RFG, the change is continuous!

3. The transverse momentum and the contour plots of the post FO distribution

The third set of figures, Figs. (11, 12, 13, 14), shows the evolution of the local transverse¹ momentum distribution and the corresponding contour plots of the post FO momentum distribution.

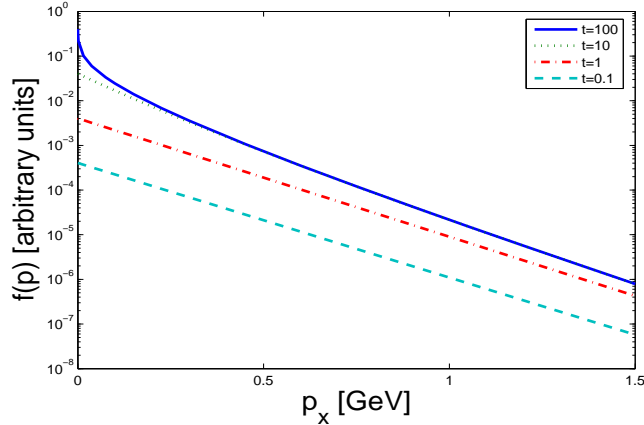


FIG. 11: The local transverse momentum (here p_x) distribution for a baryonfree and massless gas at ($p_y = 0$). The calculation was done for an infinitely long ($L = 100$), FO length, where the initial flow velocity and temperature are, $u = (1;0;0;0)_{\text{RFG}}$, and $T_0 = 170\text{MeV}$. The transverse momentum

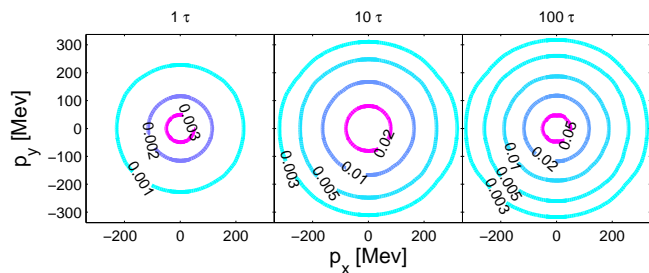


FIG. 12: The post FO distribution, $f_{\text{free}}(x;p)$, at point A of Fig. 3, for an infinitely long FO length. The figures correspond to different time points, $t = 1; 10; 100$ respectively. Contour lines are given at values represented on the figure. The initial flow velocity and temperature are, $u = (1;0;0;0)_{\text{RFG}}$ and $T_0 = 170\text{MeV}$. The maximum is increasing with t as indicated in Fig. 11.

Now, comparing Figs. (11, 12) with Figs. (13, 14), we see that the post FO momentum distributions are qual-

¹ We have presented a one-dimensional model here, but we assume that it is applicable for the direction transverse to the beam in heavy ion experiments. The plots presented should relate the transverse momentum distribution of measured particles.

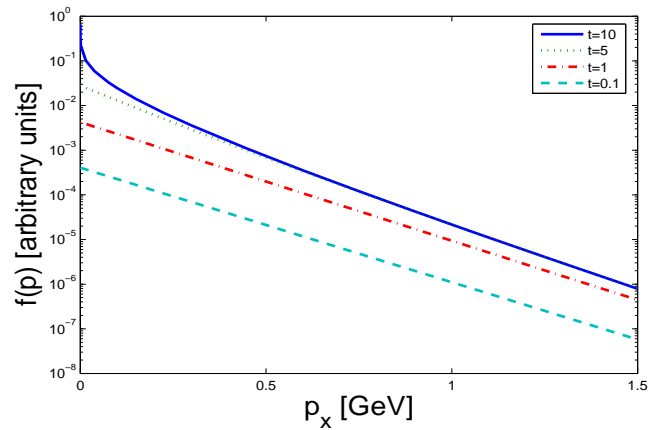


FIG. 13: The local transverse momentum (here p_x) distribution for a baryonfree and massless gas at ($p_y = 0$). The calculation was done for a finite ($L = 10$), FO length, where the

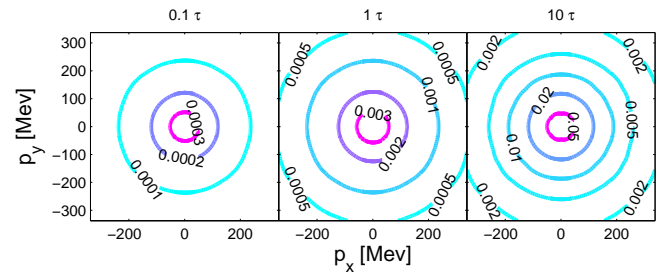


FIG. 14: The post FO distribution, $f_{\text{free}}(x;p)$, at point A of Fig. 3, for a finite FO length. The figures correspond to different time points, $t = 0.1; 1; 10$ respectively. Contour lines are given at values represented on the figure. The initial flow velocity and temperature are, $u = (1;0;0;0)_{\text{RFG}}$ and $T_0 = 170\text{MeV}$. The maximum is increasing with t as indicated in Fig. 13

itatively identical. The quantitative differences between the finite and infinite FO dynamics are small.

4. The slope of the transverse momentum distribution

The fourth set of figures, Figs. (15, 16), shows the evolution of the local transverse momentum distribution of different initial flow velocities.

Comparing the two figures, Fig. 15 with Fig. 16, our conclusion is the same as in the previous section: the results do not change much if we switch the FO description from case I to case F.

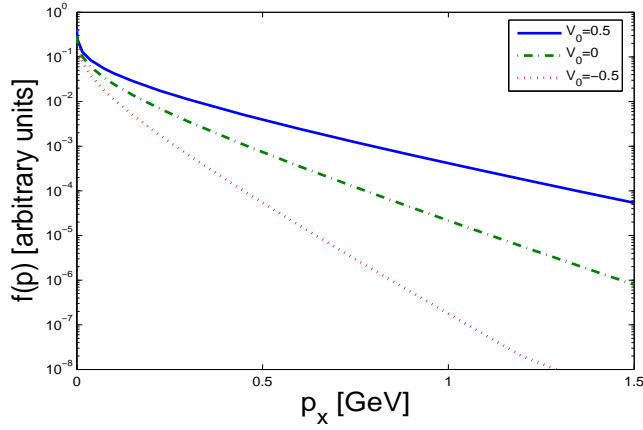


FIG . 15: The local transverse momentum distribution for a baryonfree and massless gas at $(p_y = 0)$. The calculation was done for an infinitely long, $(L = 100)$, FO length, where initial temperature is $T_0 = 170$ MeV. The values of the initial flow velocity are $u = (1; v; 0; 0)_{RFG}$, where the values of v are represented on the figure. The transverse momentum spectrum is obviously curved due to the freeze out process, particularly for large initial flow velocities. The apparent slope parameter increase with increasing transverse momentum.

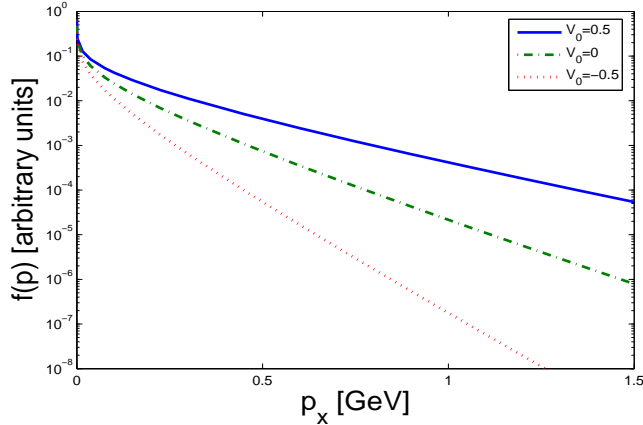


FIG . 16: The local transverse momentum distribution for a baryonfree and massless gas at $(p_y = 0)$. The calculation was done using the simple angular factor for a finite, $(L = 10)$, FO layer, where the initial temperature is $T_0 = 170$ MeV. The values of the initial flow velocity are represented on the figure.

5. The boosted post FO distribution

The fifth set of figures Figs. (17) and Figs. (18, 19), shows the boosted Juttner distribution and the final Post FO distribution corresponding to different initial flow velocities.

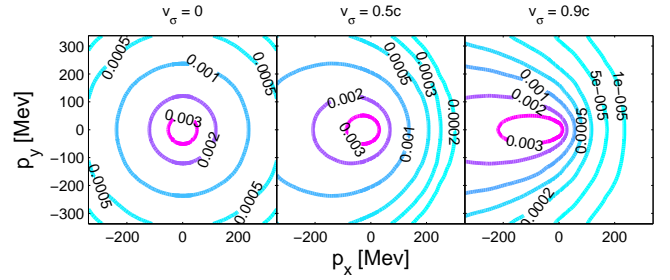


FIG . 17: The Juttner distribution at point A and boosted to the frames at points B and C as depicted in Fig. 3, and presented in the RFF frames at those points respectively. Thus, the different figures correspond to different initial normal vectors, $d = (1; v; 0; 0)$, where $v = 0; 0.5c; 0.9c$. The initial

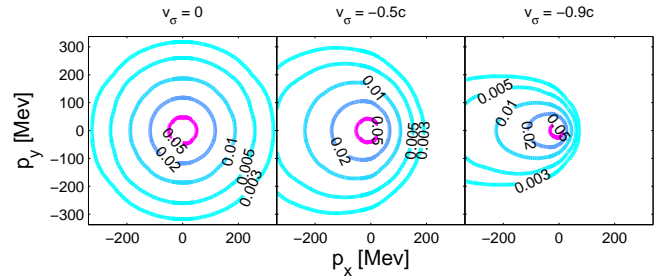


FIG . 18: The post FO distribution, $f_{free}(x; p)$, at points A, B, C of Fig. 3, in RFF, taken at infinity, $L = 300$. This is the same as the distribution at point A corresponding to different initial flow velocities, $u = (1; v; 0; 0)$, with $v = 0; 0.5c; 0.9c$ respectively and $T_0 = 170$ MeV. Note that, while the post FO distribution is a Juttner distribution at point A of Fig. 3, as $(u = d)$, the other two distributions are not boosted Juttner distributions because $(u \neq d)$, see Fig. 17. The difference is that the post FO distribution is less elongated than the boosted Juttner, because it is a superposition of sources with decreasing speed in RFF as indicated in Fig. 7.

IV . CONCLUSIONS

In this work we have presented a simple kinetic freeze out model for finite time-like layer. We have demonstrated that FO across a time-like surface in general leads to non-equilibrated unisotropic distribution. These distributions in general cannot be Lorentz transformed to a frame where the distribution is isotropic. The only exception is when the normal to the FO hypersurface is parallel to the local flow velocity. The usual practice of assuming the Juttner distribution as a post FO distribution is in general not valid!

We can also see that while the Boosted Juttner distribution is elongated in the boost direction, i.e. in the direction of d , the post FO distribution is close to a spherical and isotropic distribution at low momenta and becomes elongated only at higher momenta, see Figs.

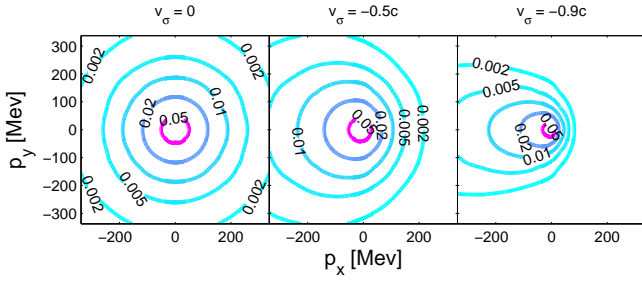


FIG. 19: The post FO distribution, $f_{free}(x;p)$, at points A, B, C of Fig. 3, in RFF, taken at finite $L = 10$, FO length. This is the same as the distribution at point A corresponding to different initial flow velocities, $u = (1; v; 0; 0)$, with $v = 0; 0.5c; 0.9c$ respectively and $T_0 = 170$ MeV. Note that, while the post FO distribution is a Jüttner distribution at point A of Fig. 3, as ($u = d$), the other two distributions are not boosted Jüttner distributions because ($u \neq d$), see Fig. ???. The difference is that the post FO distribution is less elongated than the boosted Jüttner, because it is a superposition of sources with decreasing speed in RFF as indicated in Fig. 9.

18 and 19. This special post FO distribution leads to a curved "p_z - spectrum", usually attributed to the Cronin-effect. Here we can also demonstrate (as in earlier works [8, 9]) that non-equilibrium processes in kinetic FO lead to similar effect.

We observe that the Jüttner distribution is not a good approximation for the post FO distribution just like in the case of a space-like FO. While in the case of space-like FO the Cancelling-Jüttner distribution introduced in ref. [17] is satisfactory.

Here in case of time-like FO this is not the case, and we will have to search for other simple approximations which can be applicable for a simple description of FO through a time-like surface.

V. APPENDIX

The definition of the modified Bessel function of second kind is:

$$K_n(z;w) = \frac{2^n n!}{(2n)!} z^n \int_w^{\infty} dx e^{-x} (x^2 - z^2)^{n-\frac{1}{2}}; \quad (31)$$

where if $w = z$ will lead to $K_n(z;z) = K_n(z)$ Bessel function of second kind. The indefinite integral

$$\int z^{-1} (n;z) dz = \frac{z^{-1} (n;z)}{(n+1/2)}; \quad (32)$$

where the incomplete gamma function is defined as

$$\Gamma(n;z) = \int_z^{\infty} dt t^{n-1} e^{-t}; \quad (33)$$

The analytically not integrable functions $G_n(p;m)$ and $G_n^+(p;m)$ are defined such as:

$$G_n(p;m) = \frac{1}{T^3} \int_0^{\infty} dp p \frac{p}{p^2 + m^2} e^{-p} \quad (34)$$

$$G_n^+(p;m) = \frac{1}{T^3} \int_0^{\infty} dp p \frac{p}{p^2 + m^2} e^{-p} \frac{ju}{T};$$

furthermore, the massless limit leads to:

$$G_1(p;0) = \frac{1}{T^3} \int_0^{\infty} dp p^2 e^{-p} \frac{ju}{T} p(1-ju) \quad (35)$$

$$= \frac{2}{3} (1-ju)^3;$$

$$G_2(p;0) = \frac{1}{T^3} \int_0^{\infty} dp p^3 e^{-p} \frac{ju}{T} p(1-ju) \quad (36)$$

$$= \frac{3T}{2} (1-ju)^4;$$

The general calculation of the integrals in RFF, is

$$\int_0^{\infty} dp f(p) e^{-p} \frac{p}{p^2 + m^2} e^{-ju/p} \quad (37)$$

$$= \int_0^{\infty} dz u \frac{e^{-z}}{z^2 + a^2} e^{-z} \frac{p}{z^2 + a^2}$$

$$+ \int_0^{\infty} dz u + j \frac{p}{z^2 + a^2} e^{-z} \frac{p}{z^2 + a^2};$$

where, $z = \frac{p}{p^2 + m^2} - ju/p = T$, $a = m = T$ and $b = a$.

Acknowledgments

Some authors, L.P.C semai, A.Nyiri, K.Tamosiunas and E.Molnar, thanks the hospitality of the University of Cape Town where parts of this work were done.

E.Molnar, thanks the hospitality of the Babes-Bolyai University of Cluj, where parts of this work were done.

Enlightening discussions with Cs.Anderlik, R.Adam, S.S.Wheaton and T.S.Biro are gratefully acknowledged.

[1] L.D.Landau, Izv.Akad.Nauk SSSR 17, 51 (1953)
 [2] L.P.C semai, Sov.JETP 65 (1987) 216; Zh.Eksp.Theor. Fiz. 92 (1987) 379.
 [3] F.C Cooper and G.Frye, Phys. Rev. D 10 (1974) 186.

[4] K.A.Bugaev, Nuclear Phys. A 606 (1996) 559.
 [5] L.P.C semai, Zs.Lazar, D.Molnar, Heavy Ion Physics, 5 (1997) 467-474.
 [6] L.P.C semai, V.K.Magas, E.Molnar, A.Nyiri and K.

- Tam osiunas, hep-ph/0406082.
- [7] C s. A nderlik, Z s. Lazar, V . K . M agas, L . P . C semai, H . Stocker and W . G reiner, Phys. Rev. C , 59 (1999) 388.
- [8] V . K . M agas, C s. A nderlik, L . P . C semai, F . G rassi, W . G reiner, Y . H am a, T . K odam a, Z s. Lazar and H . Stocker, Heavy Ion Physics, 9 (1999) 193-216.
- [9] V . K . M agas, C s. A nderlik, L . P . C semai, F . G rassi, W . G reiner, Y . H am a, T . K odam a, Z s. Lazar and H . Stocker, Phys. Lett. B , 459 (1999) 33-36.
- [10] V . K . M agas, A . A nderlik, C s. A nderlik and L . P . C sernai, Eur. Phys. J. C 30 (2003) 255-261.
- [11] E . M olnar et al. (2005) "C ovariant description of kinetic freeze out through a nite space-like layer".
- [12] L . P . C semai et al. Proceedings, hep-ph/0401005.
- [13] R . Balescu, Equilibrium and nonequilibrium statistical mechanics (W iley and Sons, 1975)
- [14] R . Balescu, Statistical Dynamics (Im perial College Press, 2000)
- [15] V . K . M agas, Talk at the 4th Collaboration Meeting on Atomic and Subatomic Reaction Modeling + BCPL User Meeting, Trento, Italy, February 26-29, 2004.
- [16] V . K . M agas, Talk at the International Workshop "Creation and Flow of Baryons in Hadronic and Nuclear Collisions", Trento, Italy, May 3-7, 2004.
- [17] K . Tam osiunas and L . P . C semai, Eur. Phys. J. A 20 (2004) 269-275.